JOURNAL OF GEOPHYSICAL RESEARCH, VOL. 99, NO. D8, PAGES 16,815–16,829, AUGUST 20, 1994

Characteristics of stratosphere-troposphere exchange in a general circulation model

Philip W. Mote[1] and James R. Holton
Department of Atmospheric Sciences, University of Washington, Seattle

Byron A. Boville
National Center for Atmospheric Research, Boulder, Colorado

Abstract. Air and trace gases are exchanged between the stratosphere and the troposphere on a variety of scales; but general circulation models (GCMs) are unable to represent the smaller scales. It would be useful to see how a GCM represents stratosphere-troposphere exchange (STE), both to identify possible model deficiencies which would affect other studies and to see how important the smaller-scale physics might be in the atmosphere itself. Our understanding of observed STE depends largely on inferences from tracer distributions. In this study we examine mass exchange, water vapor exchange, and the behavior of idealized tracers and parcels to diagnose STE in the National Center for Atmospheric Research GCM, the Community Climate Model (CCM2). The CCM2 correctly represents the seasonality of mass exchange across 100 hPa, but values are uniformly too strong. Water vapor, however, indicates that tropical STE is not well represented in the CCM2; even though mean tropopause temperatures are colder than observed, the lower stratosphere is too moist. Most net mass flux occurs at water vapor mixing ratios of about 4-5 parts per million by volume (ppmv), about 1 ppmv too moist. Vertical resolution has little impact on the nature of tropical STE. In midlatitudes, CCM2 more successfully represents STE, which occurs in developing baroclinic waves and stationary anticyclones. Exchange from troposphere to stratosphere does occur but only influences the lowest few kilometers of the extratropical stratosphere, even for tracers with large vertical gradients.

1. Introduction

Prior to the late 1940s, it was generally assumed that the stratosphere was in radiative equilibrium and its composition affected only by diffusion up from the troposphere [*Brewer*, 1949]; this was a one-dimensional view of stratosphere-troposphere exchange (STE). But in analyzing water vapor measurements over England, Brewer concluded that the observed mixing ratios were considerably lower than the minimum saturation mixing ratios at the local tropopause, while the upward-diffusion model would imply mixing ratios equal to the local minimum saturation mixing ratio. He proposed that instead stratospheric air in midlatitudes must have entered the stratosphere in the tropics, where the tropopause was sufficiently cold to explain the observed mixing ratios, and then drifted slowly poleward, a two-dimensional picture of STE. *Dobson* [1956] showed that such a poleward and downward circulation was consistent with the high ozone values found in the midlatitude lower stratosphere.

The quest for tropopause-level temperatures "sufficiently cold to explain observed mixing ratios," known as the "cold trap," has guided much research on STE. The very dry lower stratosphere, by inference, sharply limits the location and season of mass transfer from troposphere to stratosphere [*Holton*, 1984]. Thus although annual mean, zonal mean tropical tropopause temperatures are too warm to explain observed lower stratospheric water vapor mixing ratios, the cold trap condition is met at some times and locations. *Newell and Gould-Stewart* [1981], in an analysis of tropical radiosonde 100 hPa data, identified northern hemisphere winter and the western Pacific as the most probable time and location for troposphere-stratosphere mass transfer to occur; they termed this the "stratospheric fountain." *Robinson and Atticks Schoen* [1987] compiled statistics using radiosonde measurements of saturation mixing ratios at 100 hPa and at the profile minimum temperature. The observations occurred in intensive observing periods during the FGGE year (fall 1978 to summer 1979) between 20°S and 20°N. Their results essentially confirmed those of Newell and Gould-Stewart but also indicated the degree of variability on short time and spatial scales and showed that the minimum saturation vapor pressure often occurred well above 100 hPa.

In the troposphere the tropical rising motion implied by the Brewer-Dobson circulation does not take the form of slow ascent over a broad area, as this would cause widespread cirrus cloud, which is not observed. Instead, most ascent takes place as convection. It is no coincidence that the restrictions on times and locations of STE imposed by the requirement that

[1]Now at U.K. Universities' Global Atmospheric Modeling Programme (UGAMP) and Department of Meteorology, University of Edinburgh, Scotland.

Paper number 94JD00913.
0148-0227/94/94JD-00913$05.00

convection be the dominant agent are the same as those imposed by the requirement that air pass into the stratosphere under conditions of low water vapor mixing ratios, the "cold trap" discussed above. Moist adiabatic ascent in deep convection rapidly cools parcels, removing water by condensation; with sufficient buoyancy such parcels can penetrate the tropopause and enter the stratosphere.

Johnston and Solomon [1979], *Danielsen* [1982], and *Kley et al.* [1982] focused on the role of thunderstorms in injecting dry air into the stratosphere. If thunderstorms dehydrate the tropical lower stratosphere, then mass transfer into the stratosphere must take place predominantly on occasions when clouds penetrate the tropopause and reach very low temperatures, since they bring saturated air and some ice. Mass transfer to the stratosphere in convective clouds would require, furthermore, that most ice crystals fall out before sublimating.

Recently, the Stratosphere-Troposphere Exchange Project (STEP) team reported on a series of airborne experiments near Darwin, Australia, in January to February 1987 [*Russell et al.*, 1993]; they measured water vapor and total water, numerous trace species including ozone, aerosols, cloud condensation nuclei and radiation near to, above, and far from tropical convective clouds and tropical cyclones. *Danielsen* [1993] described the differing behavior and effects on the lower stratosphere of convection forming entirely over the ocean, of convection in air with both continental and maritime origins, and of tropical cyclones. *Selkirk* [1993] showed that in most radiosonde profiles, the potential temperature at the coldest point in the profile was 10-20 K greater than the surface equivalent potential temperature and that this "cold point" occurred well within a layer of stratosphere-troposphere mixing, not at its lower boundary.

In midlatitudes, exchange is quasi-horizontal and associated with synoptic-scale baroclinic waves. Measurements of high ozone amounts in the lower troposphere behind cold fronts [*Reed and Danielsen*, 1959; *Danielsen*, 1968] provided clear evidence that stratospheric air was drawn into the troposphere in "tropopause-folding" events driven by midlatitude storms. Further in situ [*Danielsen et al.*, 1987, *Browell et al.*, 1987] and satellite [*Appenzeller and Davies*, 1992] studies focused solely on downward transfer of mass. But other studies, such as those of *Kritz et al.* [1991] and *Hoerling et al.* [1993], indicate that some tropospheric air must also be injected into the stratosphere in conjunction with baroclinic waves.

The motivation for this paper is twofold. First, despite the wealth of observations as described above, many questions remain about the nature of STE. To the extent that a general circulation model (GCM) of the atmosphere represents the relevant physics, it can address these questions: such questions include whether penetrating cumulonimbus clouds in the tropics indeed dominate STE there and whether troposphere-to-stratosphere mass flux in midlatitudes is an important process, as the results of *Hoerling et al.* [1993] indicate. Second, the utility of GCMs in addressing specific issues like the effects of a fleet of high-speed civil transport aircraft on the lower stratosphere requires an adequate representation of the STE process. A close investigation of the characteristics of this process in a GCM can identify some limitations which may affect the interpretation of GCM results where STE may be important. For example, if sub-grid-scale processes like convection are crucial to STE and are inadequately represented in a GCM (as we might suspect), then STE will look quite different in a GCM.

2. Description of the General Circulation Model (GCM)

The general circulation model used in this study is the new version of the NCAR Community Climate Model (CCM2). CCM2, a global spectral model, includes a number of changes from previous versions of the CCM. It employs a shape-preserving semi-Lagrangian transport (SLT) scheme for constituent transport, a completely new convective mass-flux approach to parameterized convection, and improved treatment of clouds and radiation. A complete description may be found in the work of *Hack et al.* [1993]. Momentum sinks above the boundary layer are provided both by parameterized gravity wave drag and by Rayleigh friction in the mesosphere. We used a middle-atmosphere version of the CCM2 which extends vertically to 75 km, and as the CCM2 was under development during the early phase of this project, we used an early version (v13) and a later version (v17).

The vertical resolutions used here were L35 with roughly 2.5 km spacing between levels throughout the middle atmosphere, L75 with roughly 1-km spacing, and L44 with roughly 1.5 km spacing, increasing with height. The L35 and L75 runs were performed using a horizontal resolution of triangular-31 (T31) resolution, approximately 3.75° x 3.75°, and the L44 run used a trapezoidal truncation with 42 meridional and 21 zonal waves (T42x21), approximately 2.8° x 5.6°. The L75 run was initialized with fields from the L35 run, and adjustment of temperature near the tropical tropopause took approximately 3 months. In the L75 and L44 runs, Rayleigh friction was increased above 50 km to combat a model proclivity for higher wind speeds at higher vertical resolutions.

The longer simulations included methane, which was converted to water vapor in the stratosphere using photochemical loss rates from the two-dimensional model of *Garcia and Solomon* [1983]. *Boville et al.* [1991] discussed a simulation of the Mount Pinatubo aerosol cloud, in which a quantity of tracer was injected at 24 km at the grid point nearest Mount Pinatubo on June 15 of a model year and advected as a passive tracer for 180 days. This tracer, with its large spatial gradients, emphasizes transient dispersive processes and resembles episodic inputs like bomb blasts. Idealized stratospheric ("strat") and tropospheric ("trop") tracers were initialized as single-level, zonally uniform rings at 50 and 350 hPa, respectively. The initial (January 1) meridional distribution of the tracers varied smoothly from unity at the equator to 0 at (and poleward of) 30°. These tracers show how and where tropospheric air reaches the stratosphere and vice versa.

The addition of a Lagrangian parcel advection capability to the CCM2 provides a new method of investigating features of the model such as STE. The user specifies the initial positions of the parcels, and their positions are calculated at each time step using iterative interpolation between departure vector velocity and arrival velocity; this is a fully on-line trajectory scheme. In addition to position, the code interpolates pressure, temperature and water vapor mixing ratio, providing further diagnostics for model behavior along trajectories. We used the parcel code for two simulations, one to study tropical STE and one to study midlatitude STE. The details of each will be discussed below; Table 1 summarizes the model simulations discussed here.

Water vapor is the most difficult tracer to model accurately because of the strong dependence of water vapor saturation on

Table 1. Overview of GCM runs

Experiment	Resolution	Duration of Run
Methane photochemistry[a]	T31L35	four years
Methane photochemistry[b]	T31L75	one year
Methane photochemistry	T42x21L44	four years
Pinatubo	T42L35	June 15 to Dec. 15
Idealized stratospheric and tropospheric tracers	T31L35	Jan. 1 to Feb. 28
Parcels-tropical	T31L35	Jan. 1-5
Parcels-midlatitude	T31L75	Jan. 19-25

[a] model version 13; other experiments used version 17
[b] no gravity wave drag

temperature. Correct representation of water vapor requires that temperature and vertical velocity be correctly correlated at a wide variety of temporal and spatial scales, not all of which are represented in a GCM; water vapor therefore poses a potential problem in a GCM and a means of identifying the importance of unresolved scales.

3. Tropical Tropopause

In this section we examine stratosphere-troposphere exchange in the tropics from two perspectives: the large-scale perspective, in which tropical STE must meet requirements as deduced from global data sets, and the small-scale, phenomenological perspective. From each perspective we will discuss observations and the characteristics of STE in the CCM2.

3.1. Large-Scale Perspective

Early efforts to explain the observed seasonality of tropopause temperatures and, by extension, mass flux through the tropopause focused on local forcing. For instance, *Reid and Gage* [1981] proposed that at perihelion the tropical oceans absorb more sunlight and supply more sensible and latent heat to the atmosphere, increasing buoyancy; with more buoyant air, convection rises to greater heights and cools the tropopause adiabatically. Although this explanation is intuitively appealing and convection peaks in January or February, sea surface temperatures reach a maximum in April [e.g., *Zhang*, 1993].

A less obvious explanation of seasonality in mass flux and tropopause temperatures is that STE in the tropics is driven by wave activity in the extratropics [Yulaeva et al., 1994]. This process, referred to as "nonlocal control," can best be understood by considering the transformed Eulerian mean (TEM) form of the zonally averaged equations of motion. As shown, for example, by *Haynes et al.* [1991], the TEM momentum equation can be written

$$\frac{\partial \bar{u}}{\partial t}+\left[\frac{1}{a\cos\phi}\frac{\partial}{\partial\phi}\left(\bar{u}\cos\phi-f\right)\right]\bar{v}^{*}+\frac{\partial \bar{u}}{\partial z}\bar{w}^{*}=\bar{X}+\frac{1}{\rho_o}\nabla\cdot\vec{F}$$

where $\bar{u}$ is the zonal wind, $\bar{v}^{*}$ and $\bar{w}^{*}$ the TEM meridional and vertical velocities, respectively, $\bar{X}$ the damping by unresolved friction and small-scale waves, and $\nabla\cdot\vec{F}$ the Eliassen-Palm flux divergence, which represents the zonal drag of dissipating planetary waves. The reasoning is straightforward: the dissipation of large-scale extratropical waves and gravity waves appears as a negative zonal force on the right side, and the equation may be balanced if any term on the left becomes sufficiently negative. Scale analysis shows that, in general, it must be the Coriolis acceleration due to the residual meridional velocity that balances the wave drag. Since the term in brackets is negative in the northern hemisphere and positive in the southern, poleward flow is required to provide the balance. Continuity implies subsidence poleward of the maximum in poleward mass flux and ascent equatorward of that. Hence the strength of the residual circulation depends directly on the remote forcing by breaking waves, and mass flux through the tropical tropopause is governed by extratropical wave activity.

The observed seasonal evolution of STE has been studied by *Holton* [1990] and *Rosenlof and Holton* [1993], who used the nonlocal control method to estimate downward mass fluxes through the 100-hPa surface in the extratropics, thereby inferring the tropical upward fluxes required for mass continuity. Using Rosenlof and Holton's nonlocal control estimates, upward fluxes are largest (114 x 10^8 kg/s) during December-January-February (DJF) and smallest (56 x 10^8 kg/s) in June-July-August, consistent with the argument above, given that planetary wave activity is greatest in northern winter [e.g., *Randel*, 1992, pp. 197-200]. The area of upwelling is smallest (15°S to 15°N) in DJF and largest (45°S to 15°N) in September-October-November. Within the large region of upward flux, Rosenlof and Holton's approach gives no information about the spatial distribution of mass flux; *Hoerling et al.* [1993], however, calculated the horizontal distribution of mass fluxes through the tropopause.

Because the observed large-scale mass flux is greatest in DJF, we will emphasize that season. The greatest mass flux coincides with the period of minimum 100 hPa temperatures over the western Pacific and Indonesia [*Newell and Gould-Stewart*, 1981], with a maximum in convective activity there [*Zhang*, 1993] and with minimum zonal mean water vapor mixing ratios in the tropical lower stratosphere [*Rind et al.*, 1993].

3.2. Small-Scale Perspective

Convection, as mentioned above, plays an important role in the maintenance of the tropical tropopause; the areas where temperature minima occur coincide with areas of greatest convective activity. Many factors point to convection as the agent of transport between troposphere and stratosphere. Convective turrets have been observed to penetrate well into the stratosphere, providing a mechanism of direct injection of tropospheric air. Aircraft observations over Panama in 1980 [*Kley et al.*, 1982] indicated that convection was locally hydrating the stratosphere; that is, the minimum saturation mixing ratio was considerably greater (and 2 km lower) than the actual minimum mixing ratio. The existence of a water vapor minimum above the tropopause, or "elevated hygropause," suggests that air somewhere has been transported above the altitude of the local tropopause while being dried to a water mixing ratio lower than exists at the local tropopause and that this driest air dominates the tropical lower stratosphere.

The most convincing evidence that convection is the primary agent of tropical STE came from the STEP experiment in January to February 1987. Detection in the stratosphere of radon, a short-lived gas whose primary source is the land surface, in conjunction with low total water near cirrus anvils,

provided clear indication that convection transports air rapidly from the surface into the lower stratosphere [*Kritz et al.*, 1993]. *Kelly et al.* [1993] reported that on one flight over Darwin, Australia (January 13, 1987), cloud was present up to 1.1 km above the tropopause. From 17 km, just above the tropopause, to 19 km, well above the cloud top, ozone mixing ratio and cloud condensation nuclei (CCN) varied fairly smoothly from their tropospheric value to their lower stratospheric value, indicating a mixing zone which lay entirely in the stratosphere. This suggests that convective input of mass and trace constituents to the stratosphere can alter the properties of a fairly deep layer of the lower stratosphere, even above the cloud itself.

If convection transports air with low saturation mixing ratio into the stratosphere, it must simultaneously be depleted of ice crystals, otherwise the additional water would sublimate in unsaturated regions and result in hydration. *Holton* [1984] termed this the "water vapor puzzle". *Danielsen* [1982] proposed a mechanism by which cirrus anvils could become dehydrated before the air they contain could be mixed with stratospheric air: radiative heating below and cooling above could destabilize the anvil, providing mixing which would allow the ice crystals to aggregate and attain sizes great enough to fall. *Robinson and Atticks Schoen* [1987] reported, however, that not one of the 16,000 radiosonde ascents they examined resembled the thermal structure required by Danielsen's hypothesis. *Danielsen* [1993] showed one profile taken by the ER-2 aircraft during the STEP experiment which closely resembled his predicted curve, adding some credibility to his hypothesis. Direct measurements by *Knollenberg et al.* [1993], however, indicated that most of the ice rapidly fell out, since many particles were quite large and even the small ones had considerable fall speeds.

Tropical cyclones may also play a significant role in mass transfer from troposphere to stratosphere [*Danielsen*, 1993]. They appear to do so by a mechanism different from the direct injection in cumulonimbus clouds: by lifting a broad layer of tropopause-level air and depositing it, relatively unmixed, in the stratosphere.

3.3 Modeled Tropical Tropopause: Large Scale

As mentioned in section 3.1, Rosenlof and Holton [1993] calculated seasonal variations in cross-100 hPa mass flux using UKMO data; they performed the same calculation on CCM2 output from one year of a T31L35 integration, and K.H. Rosenlof [personal communication, 1992] repeated the calculation on one year each of T42L44 and T31L75 integrations. Table 2 summarizes the upward mass fluxes they calculated, both in absolute terms and as a percentage of the annual total. At all configurations used here, the CCM2 tends to have larger fluxes (by about 60%) and larger areas of upwelling than in the Rosenlof and Holton's estimates for the atmosphere, but the seasonality in the model resembles that in the data as indicated by the percentage of annual flux (except that the difference between DJF and MAM is too small). The strength of the circulation diminishes rapidly with height in the lower stratosphere and is generally weaker than observed in the middle and upper stratosphere.

The model tropopause tends to be somewhat colder than observed and to occur above 100 hPa. With L35 vertical resolution the tropopause is at 99 hPa and adjacent levels are at 140 and 70 hPa; with L44 the tropopause is at 86 hPa and adjacent levels are at 105 and 71 hPa; and with L75 the tropopause is at 85 hPa and adjacent levels are at 99 and 74 hPa. A 4-year average of European Centre for Medium-Range Weather Forecasting (ECMWF) data at 100 hPa compared to four years of CCM2 output (at T31L35) interpolated to 100 hPa shows the CCM2 to be generally 1-3 K too cool in the tropics (Figure 1). At higher vertical resolutions (not shown) the (interpolated) 100-hPa level is warmer, with an area mean temperature close to that of observations even though the tropopause itself is cooler.

Table 2. Comparison of 100 hPa Tropical Mass Flux forCCM2 and Observations

	Seasonal Fluxes x10^8 kg s^{-1}, Annual x10^8 kg yr^{-1}, % of Annual Total							
	L35		L44		L75		Observed	
Season	Flux	%	Flux	%	Flux	%	Flux	%
DJF	157	31	162	33	130	26	114	36
MAM	146	29	141	29	136	27	76	24
JJA	90	18	79	16	98	19	56	18
SON	112	22	109	22	141*	28*	70	22
Annual	3.98		3.87		3.98		2.49	

CCM, Community Climate Model. DJF, December-January-February; MAM, March-April-May; JJA, June-July-August; SON, September-October-November.

*Includes October and November only, since vertical resolution changed at the beginning of September.

In January the L35 model's 99-hPa mean water vapor mixing ratio (Figure 2) has low values in tropical convective regions, but southeast of each area (South America, Africa, and the maritime continent) lies an area of rather high water vapor mixing ratio (>5 parts per million by volume (ppmv)). *Rind et al.* [1993] show a comparable figure from the Stratospheric Aerosol and Gas Experiment II (SAGE II), an average of 4 years of water vapor at 100 hPa. The patterns are similar near the equator, but SAGE II mixing ratios are lower throughout the tropics and subtropics, especially southeast of each dry area.

The results of *Newell and Gould-Stewart* [1981] imply that dry air entering the stratosphere in the "stratospheric fountain" should dominate the lower stratosphere. In the CCM2 this appears to be the case (Figure 3); the dry air (3.2 ppmv) at about 150°E appears to be lifted and advected westward above considerably higher mixing ratios (which do not appear to influence the stratosphere), and the minimum at about 25 km (3.53 ppmv) is only slightly more moist. Yet mean lower stratospheric tropical mixing ratios in the CCM2 are higher than observed (figures not shown), even though the CCM2 underestimates mean tropopause temperatures.

Evidently, adequately low mean tropopause temperatures are not a sufficient condition for an adequately dry lower stratosphere; perhaps temporal variance is another necessary condition. *Frederick and Douglass* [1983] calculated that 36% of daily January (1972-1979) observations at Guam (144°E, 13°N) had 100-hPa temperatures below 189.8 K, and at Koror (134°E, 7°N) the frequency was 46%. By contrast, in the CCM2, low temperatures are much rarer. By contrast, in the CCM2, low temperatures are much rarer. Figure 4 shows the fraction of days during one model January when the 99 hPa temperature was below 189.8 K; the largest value, at about

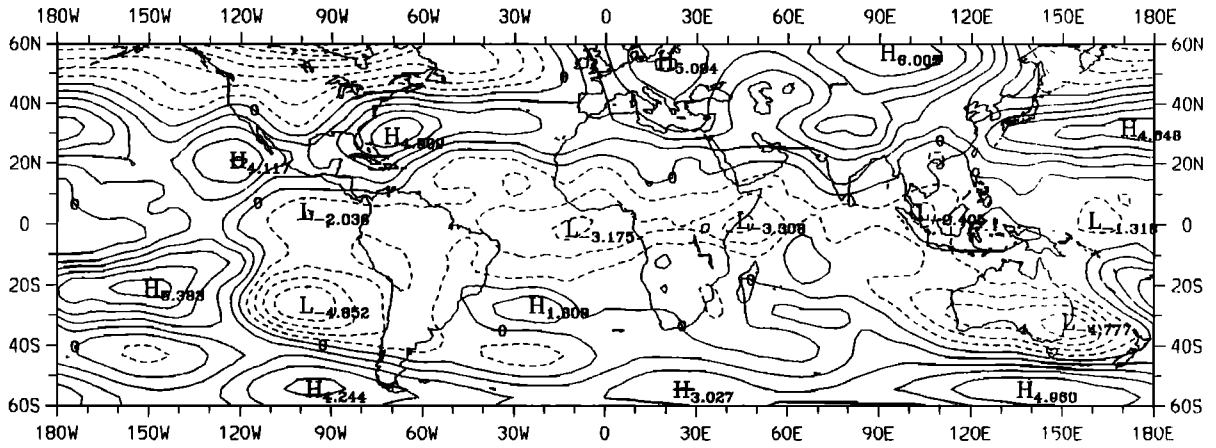

Figure 1. Difference in January mean temperature at 100 hPa between 4 years (1986-89) of European Centre for Medium-Range Weather Forecasting (ECMWF) data and 4 years of CCM2 output at T31L35 resolution. Dashed contours indicate where CCM2 is colder than ECMWF.

150°E, 5°S, is 30%, and the values at Guam and Koror are only 8% and 12%, respectively. Perhaps CCM2 percentages are lower because the CCM2 saves daily mean temperatures, thereby masking subdiurnal variations which would influence twice-daily observations. An examination of a model run with 3 hourly output shows that this is not the case; variance of tropopause-level temperature is much greater at supradiurnal than at subdiurnal frequencies.

As another approach, let us consider the relationship between vertical velocity and moisture. The tropical tropopause acts as a source of dry air for the stratosphere, since mixing ratios are lower there than anywhere. Consequently, the mean moisture flux $\overline{wq}$ must be negative, and since $\overline{wq}$ is positive in the tropics, the transient water vapor transport term $\overline{w'q'}$ should be negative, and we expect large mass transfer w to be associated with low q. A scatterplot of w and q should have negative slope, but as shown in Figure 5, the points are tightly clustered near the mean values, with few outliers and no obvious negative correlation. Few points are drier than 3 ppmv; but at those points, mean vertical velocity is negative (Figure 6a), except at the few driest points; average vertical velocity increases with increasing mixing ratio. Furthermore, virtually all net upward mass transfer takes place where the mixing ratio is greater than 4 ppmv (Figure 6b).

Low mixing ratios, then, are associated with large upward or downward vertical motions, but for low mixing ratios the net mass flux is small due to the small number of points and to the cancelation of large opposite fluxes. Rapid descent is often associated with low mixing ratio because rapid descent usually occurs at grid points adjacent to rapid ascent, as will be discussed below. Under conditions where vertical velocity is positive, however, the water vapor mixing ratio declines with increasing vertical velocity, and the points with strongest vertical motion have the lowest mean mixing ratio and are all very close to saturation. Thus while the model does produce the expected association between strong ascent and lowest mixing ratios, local circulations return much of that very dry air to the troposphere.

The addition of a model level around 85 hPa, as in the L44 and L75 resolutions, results in a colder tropopause and lower mean water vapor mixing ratios, but by other measures, STE is less well simulated at higher resolution. Although the seasonal cycle in mass flux (Table 2) and tropopause-level mixing ratio (not shown) are similar, the longitudinal variations

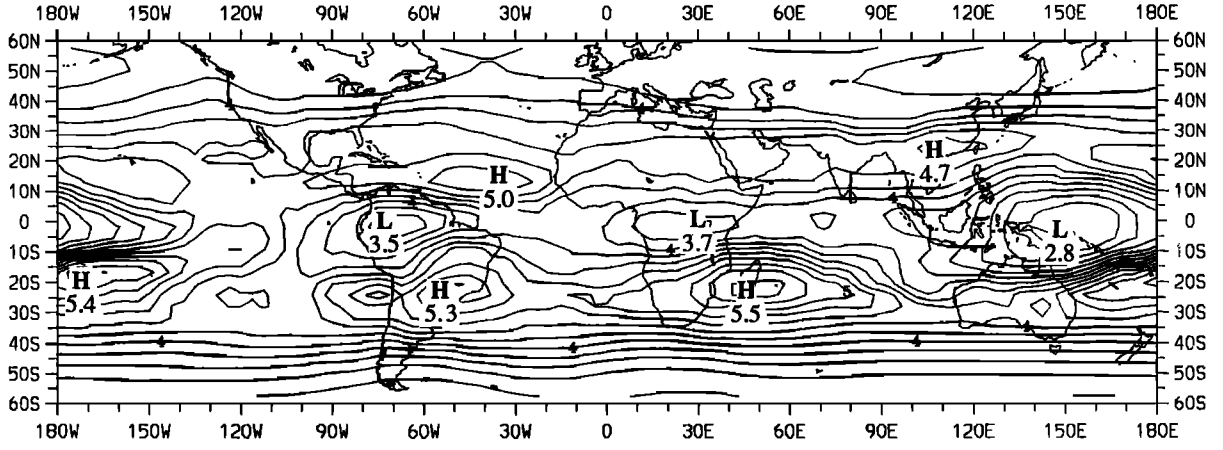

Figure 2. January mean water vapor mixing ratio, parts per million by volume (ppmv), at 99 hPa for 4 model years (T31L35).

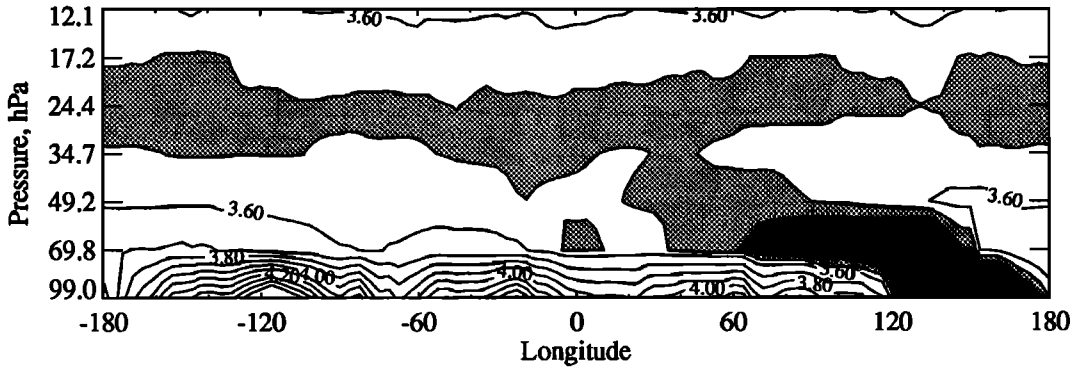

Figure 3. Meridional average from 10°S to 10°N of the model's water vapor mixing ratio (ppmv) in January, L35. Heavy (light) shading indicates mixing ratio below 3.50 (3.55) ppmv.

characteristic of the stratospheric fountain are diminished. Scatterplots of vertical velocity and water vapor analogous to Figure 5 have fewer outliers in all directions, but as in Figure 6, most mass flux still occurs at moderate mixing ratios. In short, at higher resolution, both the mean and the variance of temperature, water vapor, and vertical velocity are reduced.

3.4. Modeled Tropical Tropopause: Small Scale

Convection in the CCM2 is parameterized using a convective mass flux scheme [Hack, 1994]. Mass, tracers, and moist static energy are transported from one layer to the next and detrained in the lowest stable layer. Condensation occurs when air is saturated with respect to water or ice, as appropriate, and immediately results in precipitation. The mass transport by parameterized convection drops sharply above the middle troposphere and rarely reaches the tropopause. In the model, therefore, parameterized convection plays only a miniscule role in mass transfer to the stratosphere compared to resolved-scale vertical motions. The latter resemble convection in that they produce considerable precipitation, tend to be deep features, and have a vertical velocity maximum in the middle troposphere.

The model occasionally produces features that look somewhat like mesoscale convective complexes: one or several grid points have large upward vertical motions, covering an area as large as 1 million km^2, while surrounding grid points have large negative vertical motions. A particularly vigorous such event occurred in January of the third year of integration and lasted about 3 days while propagating southeastward over New Guinea. It generated nearly 50 cm of rain at one grid point and produced 99 hPa mixing ratios as low as 0.61 ppmv. In addition, it clearly impacted the 70 hPa water vapor distribution, although this occurred about one day later and was not directly produced by convection.

Resolved vertical motions near the tropopause during this event were as large as 11 cm s^{-1}, (Figure 7a) and sub-grid scale convection produced vertical motions as large as 1 cm s^{-1} (Figure 7b). (The field plotted in Figure 7b is the upward mass flux of the convective scheme, interpolated between the half-level below and the half-level above 99 hPa. The convective scheme produces no net mass flux, so that the upward and downward fluxes are equal at each grid point.) Around the area of ascent was a ring of subsidence, a frequent companion of strong ascent; in this case, the downward mass flux in the ring of subsidence somewhat exceeded that of the area of ascent. Generally, the 99-hPa and 70-hPa vertical velocity fields were approximately out of phase near vigorous convection, a phenomenon observed in radar data by *Balsley et al.* [1988]. While this could be due to the radiative effects of a large convective cloud deck shielding the lower stratosphere from the upward flux of infrared radiation emitted by the surface and lower troposphere and producing subsidence [*Doherty et al.*, 1984], the subsidence seems to be a consequence of strong cooling produced directly by the convective scheme; the radiative terms in the thermodynamic equation are an order of magnitude smaller.

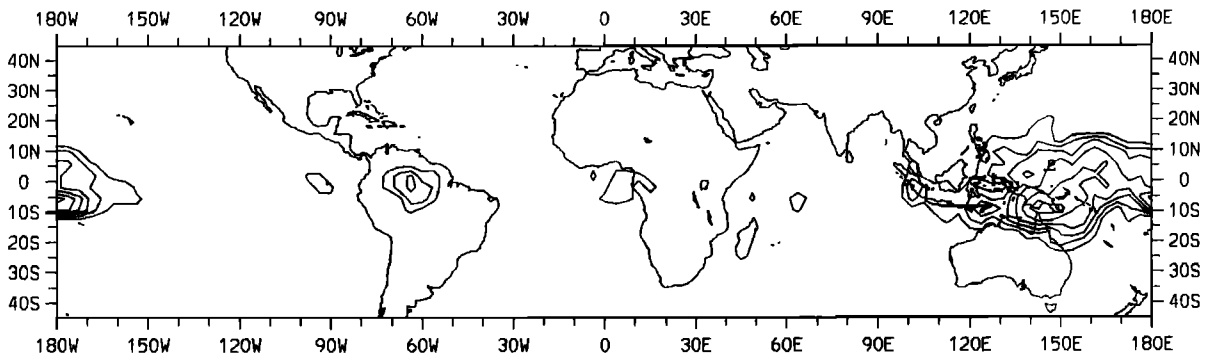

Figure 4. Frequency of occurrence of daily mean temperatures below 189.8 K in January of the fourth year at L35. Contour interval 5%.

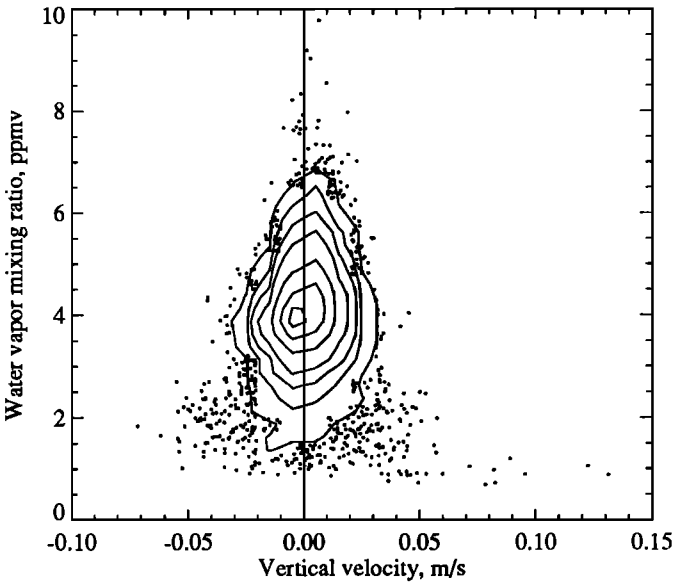

Figure 5. Scatterplot and frequency distribution of vertical velocity (0.01 m s^{-1} bins) and water vapor mixing ratio (0.5 ppmv bins) for daily mean values at 99 hPa between 15°S and 15°N in January (L35). Bins with more than 15 points are contoured by frequency; 97.5% of all points lie within the outer contour.

To examine the effect of such mesoscale vertical motion patterns at the tropopause on trace constituent exchange, it is useful to consider the advection of tracers in the CCM2. In the Pinatubo simulation the tracer began as a concentrated cloud in the stratosphere; easterly winds advect it around the globe in about 2 weeks, as observed [*Trepte et al.*, 1993]. In the first few days, small filaments of the tracer are drawn rapidly down into the troposphere as the cloud passes over regions of deep subsidence. These occur at only a few longitudes around the globe, namely, over India (80°E), Saudi Arabia and eastern Africa (30°-40°E), northern Africa (10°E), and the eastern Atlantic (20°-40°W). Between injection events the tropospheric portion of the cloud is rapidly drawn to higher latitudes, then advected eastward. The distribution of the tracer at 140 hPa on day 10 (Figure 8a) shows two filaments joining, after being injected at different times over Saudi Arabia and North Africa. The peak concentration occurs roughly at the junction of the two filaments and is a few orders of magnitude smaller than the maximum concentration at 24 hPa.

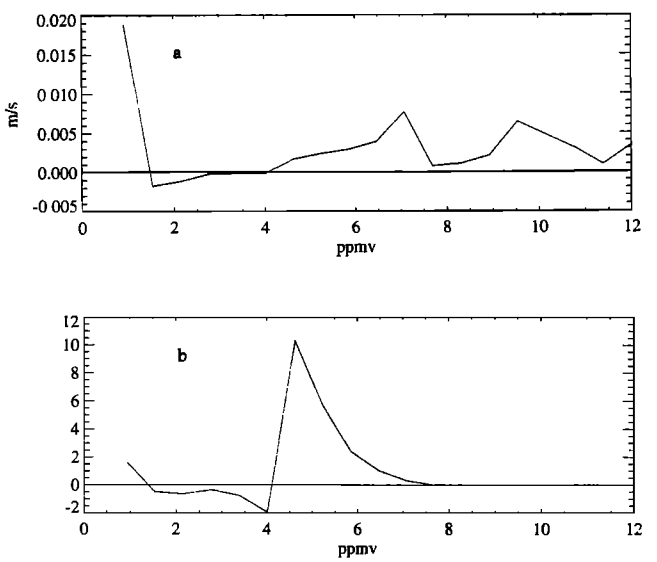

Figure 6. Plots of (a) average vertical velocity and (b) total mass flux (arbitrary units) against water vapor mixing ratio (binned at 0.5 ppmv intervals) for points as described in Fig. 5.

The transport time from the main body of the cloud down to the 140-hPa level, a vertical distance of some 10 km, is only a couple of days. This is much shorter than one would expect for grid-scale subsidence in the tropical lower stratosphere and upper troposphere. Since the semi-Lagrangian transport scheme in the CCM2 produces negligible numerical diffusion and vertical diffusion is small above the boundary layer, the rapid transport shown here must be entirely due to resolved motions.

Long-term averages of vertical velocity in the model indicate that these areas of downward motion are geographically fixed. The largest subsidence (except in southern high latitudes) for the first 30 days of the Pinatubo simulation, i.e., June 15 to July 14 (Figure 8b), occurs in a broad swath from the Indian Ocean to the Mediterranean. Positive vertical velocity features, however, are dominated by scales of 1000 km or less.

For a Lagrangian view of circulations in the vicinity of the tropical tropopause we turn now to a parcel integration using the Lagrangian code described in section 2. We initialized parcels at 2.5°x 2.5° increments around the globe between 20°N and 20°S at pressures of 70, 100, and 130 hPa on January 1 and ran the model at T31L35 resolution for 5 days. Parcel positions, temperatures, and water vapor mixing ratios were saved hourly.

The driest parcels (not shown) all began at 100 hPa in the "stratospheric fountain" region. They traveled around anticyclones in each hemisphere, the northern branch being peeled off by the winter westerlies and the southern branch coiling around Australia. From Figure 3 one might expect that the driest parcels would travel westward while rising, but evidently such motion is representative not of individual parcels but of a long-term mean. Many of the 130-hPa parcels remained in the troposphere and spread poleward, and some of the higher parcels did so as well. Of the parcels initialized at 130 hPa, 422 (17%) passed through the tropopause (100 hPa) in the 5-day period simulated; these had a mean mixing ratio of 3.1 ppmv. Twelve of these (0.5% of the total) returned to the troposphere, with minimum mixing ratios ranging from 1.2 to 3.2. By contrast, of the parcels initialized at 70 hPa, only 3.8% passed through the tropopause, with a mean mixing ratio of 2.9 ppmv. The difference between the two mixing ratios is statistically significant, but only at the 90% level; there is a somewhat higher mixing ratio for parcels rising than for parcels descending through the tropopause, and far more parcels rise than descend through the tropopause.

Similar to the Pinatubo cloud, some parcels had quite large vertical velocity, especially upward: although average potential temperature for all the parcels increased only 2.5 K, some 25 parcels had increases in potential temperature in excess of 55 K, and the most rapid rise was 50 K in one 24-hour period. All of these parcels started between 110°E and 177°W, 15°S to 15°N, approximately the "stratospheric fountain" region, and remained almost entirely within those boundaries. The cause of these large changes in potential temperature is not clear, but we suspect that the problem is with the thermodynamic calculation, which uses first-order finite differences to calculate verti-

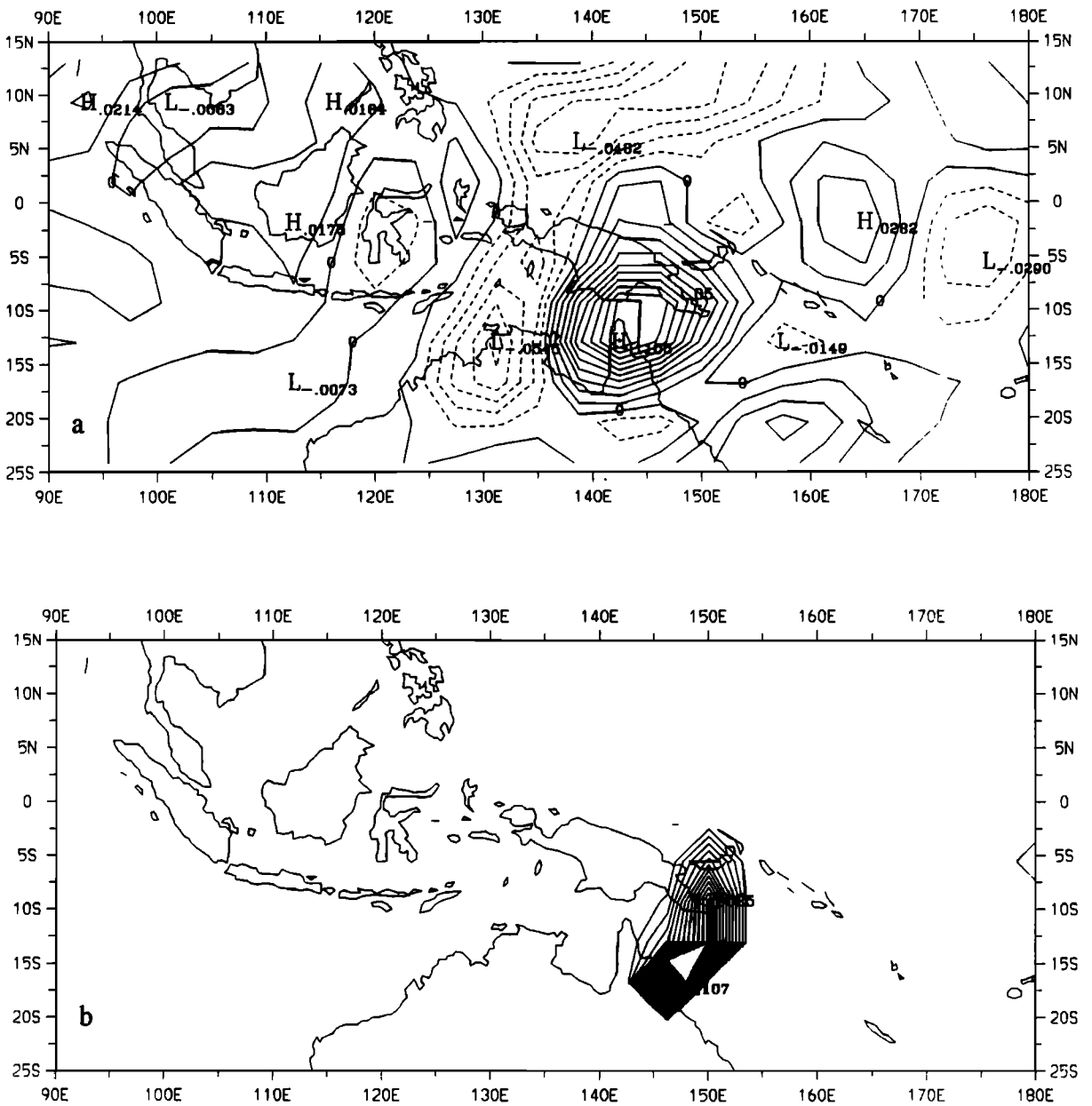

Figure 7. Vertical velocity at 99 hPa during a large convective event in January of the third year of L35 simulation: (a) resolved-scale vertical velocity and (b) equivalent upward velocity from the convective mass flux scheme. Units are centimeters per second.

cal advection, and not with the parcel code, which uses the higher-order semi-Lagrangian transport. Near the tropical tropopause, vertical velocity fluctuates at high frequency and with small vertical scale; when these vertical velocities are used to calculate parcel trajectories, large apparent changes in potential temperature could result. Scientists at NCAR are testing the use of semi-Lagrangian transport for the dynamics in CCM2, which would eliminate the problem described above.

4. Extratropical Mass Exchange

The pioneering work on midlatitude STE was accomplished by *Reed and Danielsen* [1959] and *Danielsen* [1968]. The latter study, an aircraft field experiment which measured ozone and radioactivity, conclusively showed that stratospheric air was drawn into the troposphere in long "folds" which were mixed into the troposphere. These folds were associated with baro-

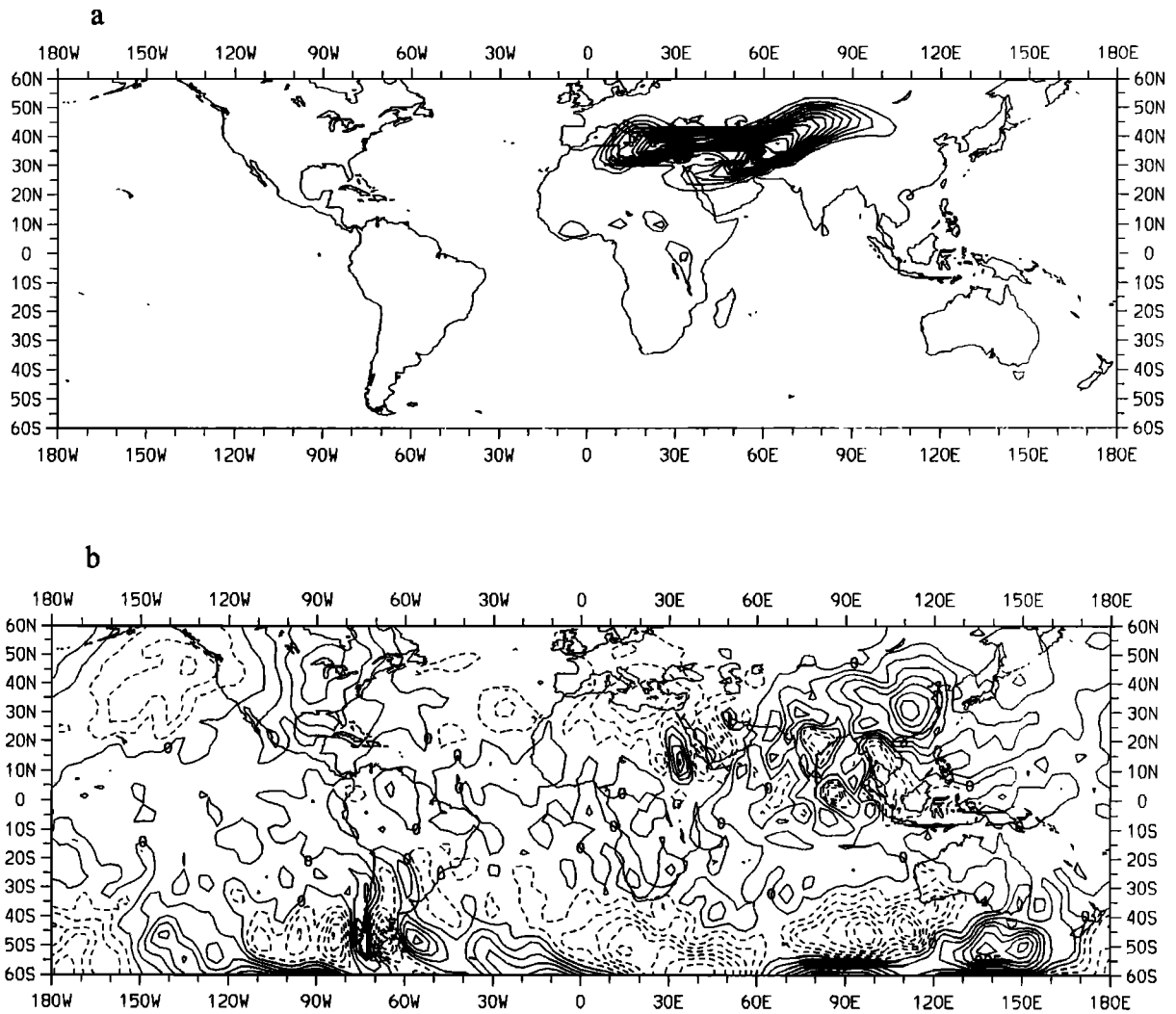

Figure 8. For the "Pinatubo" experiment, (a) Volcanic aerosol tracer at 140 hPa, day 10, and (b) mean vertical velocity at 140 hPa, days 0-29.

clinic waves, occurring behind (generally to the west of) the cold front. Danielsen envisioned a local circulation in which air was drawn into the lower stratosphere through a mixing zone to replace the mass lost in folding events.

The aridity of the stratosphere is generally taken to be evidence that little flux of air into the stratosphere occurs in midlatitudes. But *Hoerling et al.* [1993], using ECMWF analyses to calculate mass transfer across the tropopause for January 1979, found that substantial upward mass flux occurred not just in the tropics but also in the latitude bands 40°S-70°S and 50°N-70°N. At those locations the minimum saturation water vapor mixing ratio is much higher than in the tropics; large upward mass flux would flood the stratosphere with moisture. Why is this not observed?

The CCM2 can address this question, even though it does not resolve tropopause folds. Our description of the model's midlatitude STE is based on two simulations, described in part 2. In one simulation, idealized stratospheric ("strat") and tropospheric ("trop") tracers provided a mass transport view, and in the other, parcels provide an explicit Lagrangian view. Figure 9a shows the zonal mean mixing ratio of the trop tracer at the 99-hPa model level; it enters the stratosphere predominantly in the tropics, where its entry is gradual and steady. By contrast the strat tracer enters the troposphere sporadically; Figure 9b shows rapid, dominant events with maximum tracer concentration initially near 30° latitude in the northern hemisphere and 40° in the southern. As time progresses and the strat tracer spreads poleward in the stratosphere, the latitude of peak concentration in the troposphere also spreads poleward. When in the stratosphere, the trop tracer lines up approximately along isentropes and spreads slowly upward and poleward, in a manner consistent with the Brewer-Dobson circulation. Within the troposphere it seems to spread toward both poles at approximately the same rate.

On the suspicion that the strat tracer is transported into the troposphere by baroclinic waves as suggested by *Danielsen* [1968], we liken it to ozone and investigate its relationship to potential vorticity (PV) and other dynamic fields. Positive PV and negative height (not shown) anomalies are associated with strong downward motion of the strat tracer. Figure 10 shows a meridional average from 30° to 45°N of potential vorticity and the strat tracer on day 34 of integration, interpolated to pres-

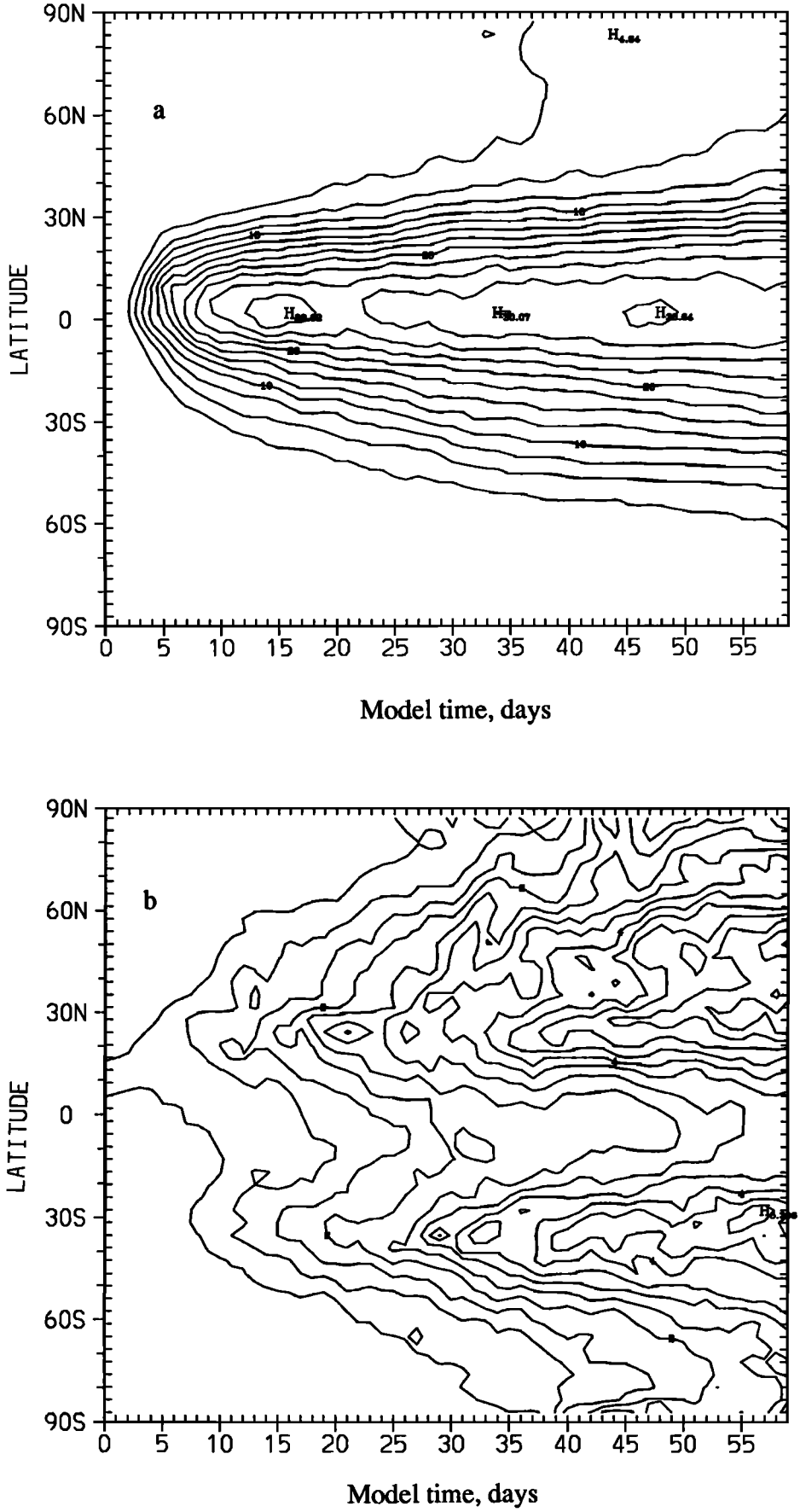

Figure 9. Zonal mean - time section of (a) the "trop" tracer at 99 hPa and (b) the "strat" tracer at 300 hPa.

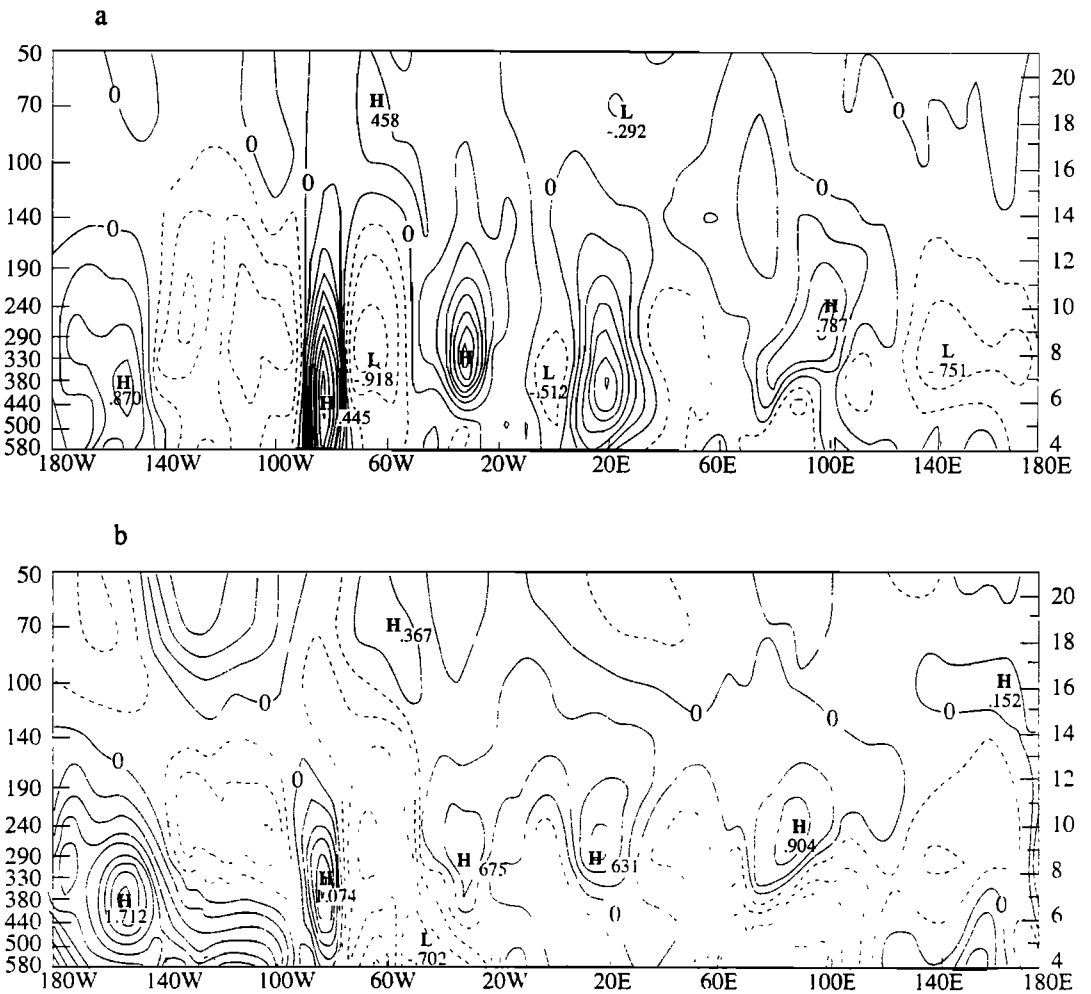

Figure 10. Cross sections averaged from 30° to 45°N of the ratio of the deviation from the zonal mean to the zonal mean itself for (a) potential vorticity and (b) the "strat" tracer. Ordinate is model pressure.

sure surfaces. The two fields are plotted as the ratio of the departure of the value from zonal mean to the zonal mean itself, in order to "see through" the strong vertical gradients and to correct for the difference in vertical gradients.

A clear correspondence between the two fields is evident between 100 hPa and 400 hPa, with five maxima and five minima. The signature of the waves extends well into the stratosphere in the height field (not shown), but it is not apparent above about 100 hPa in the strat anomaly field. One might ask whether the perturbations of these fields by tropospheric waves are associated with actual transport through the tropopause, or whether they represent reversible deformation of isentropes. In Figure 11, we show the strat tracer with potential temperature as the vertical coordinate. In the western hemisphere, there are still large positive anomalies at the same locations as in Figure 10; some tracer has crossed isentropes. Such diabatic motion indicates that transport across the tropopause has taken place.

The trop tracer sheds some light on the interesting question of midlatitude mass transfer from troposphere to stratosphere. Figure 12 shows the trop tracer displayed in the same manner as was the strat tracer in Figure 10b. Unlike the strat tracer, the trop tracer is not evidently correlated with potential vorticity and does not appear to be transported effectively into the stratosphere by baroclinic waves. There are perturbations from the zonal mean which increase rapidly with height above 100 hPa, but they are apparently associated with poleward transport from the tropics, as they coincide with maxima in the strat tracer; if they were due to upward transport, they should coincide with minima in the strat tracer. The actual values of the trop tracer in the stratosphere are quite small.

We performed flux calculations of mass and of the two tracers across vertical (in this case the 30° N latitude circle above a given level) and horizontal (190 and 100 hPa) surfaces north of 30°N. Time series of these fluxes show that at the 190 hPa model level, the net mass flux is downward, while the net trop tracer flux is upward and rather episodic on a variety of timescales. Most of the mass appears to reenter the troposphere across the midlatitude jet. In contrast the net trop tracer flux is generally downward at 100 hPa and poleward at 30° latitude above that level. The results shown here indicate that midlatitude mass flux into the stratosphere, as calculated by *Hoerling et al.* [1993], is not important for the stratosphere as a whole but only for the lowest few kilometers. This finding is consistent with numerous satellite observations of trace gases with a tropospheric source (e.g., Jones and Pyle

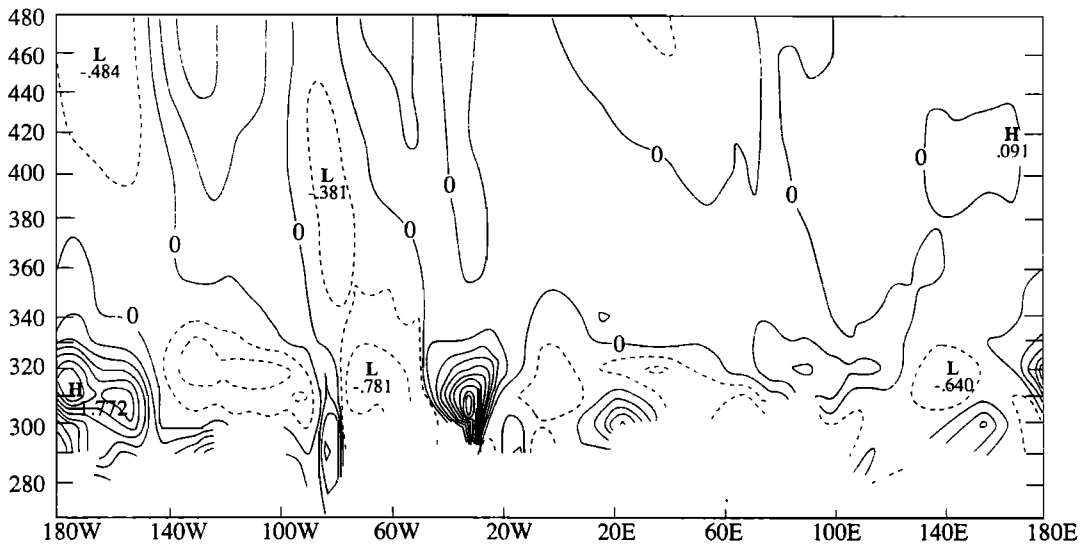

Figure 11. Vertical cross section, 30°-45°N, of the strat tracer, with potential temperature as the vertical coordinate.

[1984] for methane), which show near-tropospheric values in the tropical lower stratosphere but much lower values in the midlatitude lower stratosphere.

The Lagrangian view of midlatitude STE refines the picture presented above. We initialized parcels on January 19 of a T31L75 run, at 2.5° x 2.5° increments around the globe from 30° to 60°N, and ran for 5 days. The starting date was chosen because both area-averaged downward vertical velocity in the upper troposphere and an index of tropospheric wave activity were approaching a maximum, indicating that a maximum of STE would be occurring. The initial levels for the parcels were at values of the hybrid coordinate η equal to 0.1, 0.16, 0.22, and 0.28. The approximate pressure, in hPa, can be found by multiplying η by 1000.

Defining the model's midlatitude tropopause is considerably more difficult than defining the tropical tropopause. In the model the latter occurs at a single model level (85 hPa for the L75 model), while the former must be defined in terms of stability, potential vorticity (PV), or some other quantity, just as in the real atmosphere. Hoerling et al. [1993] used a definition of 3.5 x 10^{-6} K m^2 kg^{-1} s^{-1} poleward of 28° and a lapse rate condition (dT/dz > -2K/km) equatorward of 13°, with a smooth function joining them. Interpolating PV in both time and space to parcel positions would be prohibitively computationally intensive, so we adopted a simpler approach using water vapor, which is interpolated and stored as often as parcel positions.

Since stratospheric water vapor values are generally quite small (and vary quite little in time and space) and tropospheric values are much larger and have vastly larger ranges, water vapor has the potential for identifying parcels which pass between the troposphere and the stratosphere. Defining a boundary between the two, however, is not straightforward because their isopleths cross each other in midlatitudes. Above the extratropical tropopause, (as defined for example by *Hoerling et al.* [1993]), water vapor values can exceed typical stratospheric values by a factor of 10 or more. Such high values suggest that mass is locally exchanged between stratosphere and troposphere, and the idea of the tropopause as a material surface separating completely different air masses is inappropriate.

We cannot, therefore, define the tropopause as a particular water vapor value, but we can examine the parcel results for

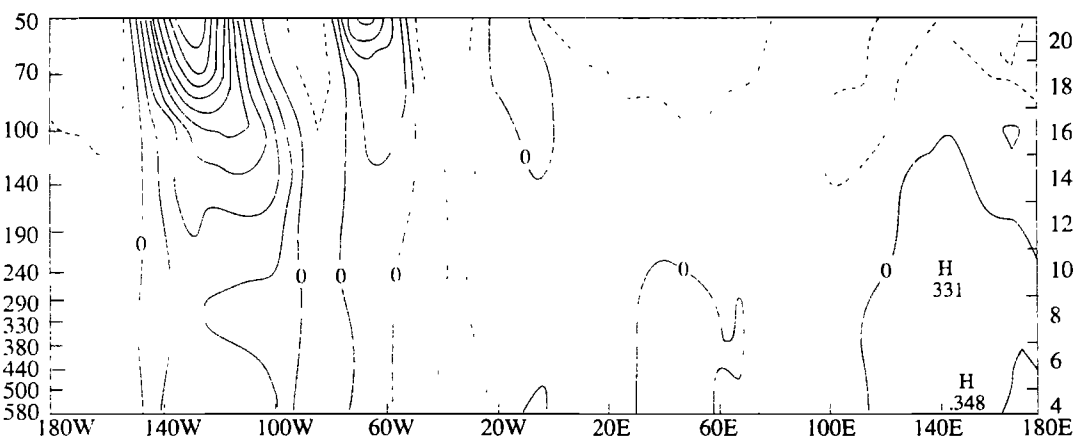

Figure 12. As in Fig. 10b but for the "trop" tracer.

large changes in water vapor mixing ratio or in height. Plate 1 shows the trajectories of those parcels initialized at h=0.22 whose downward displacement was greatest. Of all the parcels at all levels, the largest downward motion occurs in a stationary anticyclone over the central Pacific. These parcels are initially close to the tropopause, with a PV of 3.5 and a water vapor mixing ratio of 15 ppmv.

Another set of parcels that clearly crosses the tropopause is the group that begins over western Asia around 80°E. They are initially in the stratosphere, and as they approach a developing trough over the Pacific their water vapor values rise slowly from around 10 ppmv to around 20 ppmv. As they enter the trough, they plunge downward and southward, and their mixing ratios increase by 2 or even 3 orders of magnitude, the greatest change in water vapor of any parcels. Most return northward and upward, reaching much lower mixing ratios (though still characteristic of the upper troposphere) at the end of the 5-day simulation.

A cutoff low at 30°W does not seem to produce flux into the troposphere; at η=0.16, those with low mixing ratio (<8 ppmv) correspond to high PV and retain their low mixing ratio, while those with higher mixing ratio are more likely to shoot down into troposphere. Those that begin at η=0.22 behave similarly, but in this case, low mixing ratio means around 20 ppmv.

Thus while the parcel simulation indicates some role for waves in STE, the only transport which is irreversible on 1 to 2-day timescales occurs within a stationary anticyclone and west of a developing trough. No obvious cross-tropopause transport takes place in conjunction with the mature trough over the Atlantic.

5. Summary and Conclusion

Stratosphere-troposphere exchange is conventionally viewed as occurring in two dominant areas: in the tropics, where upward mass flux takes place primarily at times and locations of very low water vapor mixing ratio, and in midlatitudes, where baroclinic waves draw stratospheric air into the troposphere, and irreversible mixing takes place. The CCM2 simulations discussed here indicate that the model is capable of representing the latter process, even with fairly coarse horizontal resolution, but that the former process has a different character from the observed tropopause.

The differences between the simulated and the observed tropical tropopause are most clearly represented by the vertical motion field. The presence of very large downward as well as upward vertical motions and the association of low mixing ratios with both can produce rapid cross-tropopause transport in both directions. Unlike convective injections these continue several kilometers into the stratosphere and can be relatively stationary for a long time.

The behavior of the model's tropical tropopause as revealed by the Pinatubo simulation is rather surprising. The filaments extending into the troposphere suggest that the model's tropical tropopause is rather porous, permitting rapid downward as

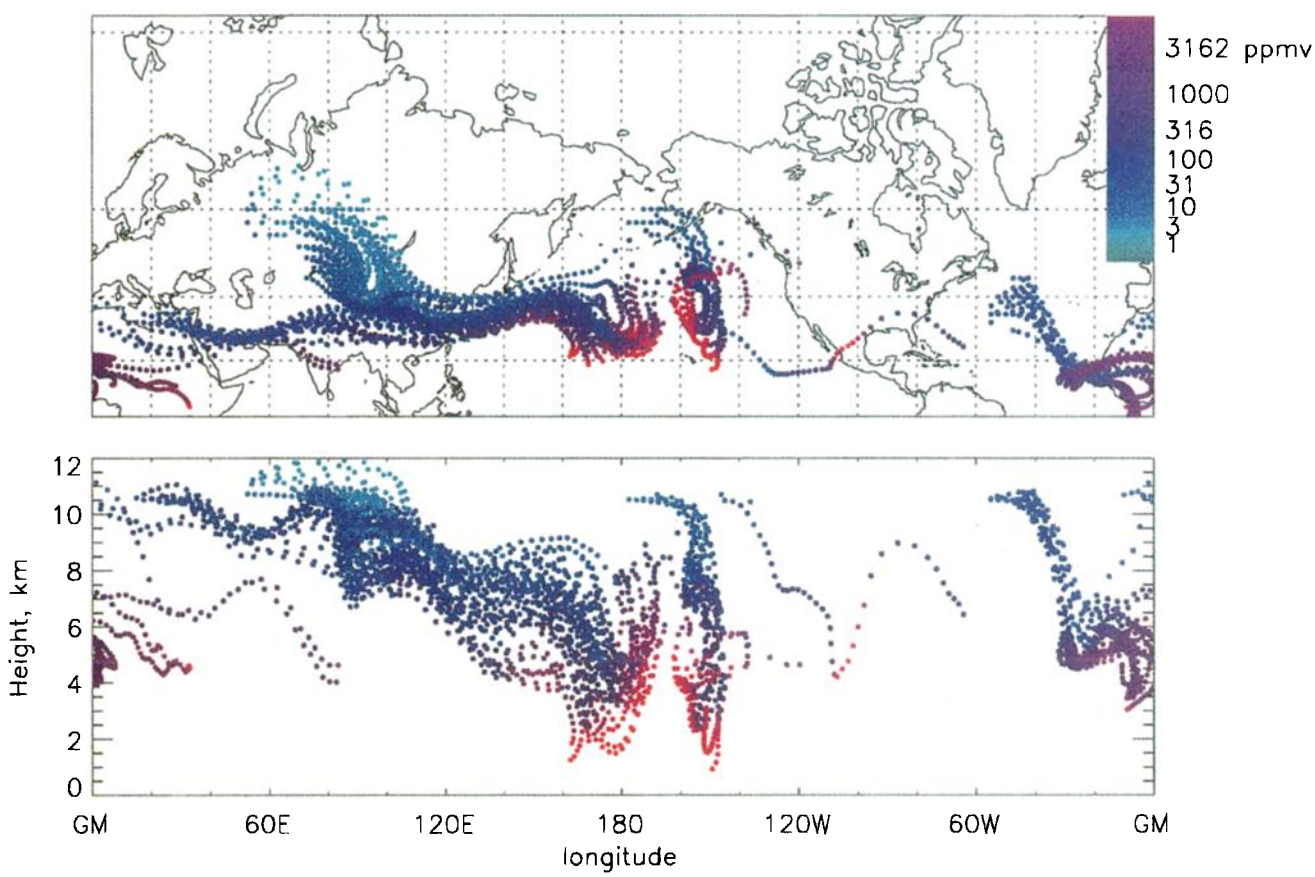

Plate 1. Trajectories of those parcels initialized at η=0.22 which descended at least 5.8 km, plotted as (a) a horizontal projection and (b) height-longitude projection.

well as upward transfer of mass and trace gases. Of course, in this experiment, the strong vertical gradient amplifies the effect of any subsidence, and the quantities of tracer drawn down are quite small. Observations of vertical motion in the real atmosphere are rare, but it seems implausible that the behavior seen in the model should be completely realistic. If the rapid downward transport evident in the Pinatubo simulation were taking place, research aircraft flights in the tropical upper troposphere should occasionally encounter ozone (or other tracer) mixing ratios characteristic of the middle stratosphere, and this has not occurred.

The large changes in potential temperature associated with these motions, as displayed by the parcel results, seem thermodynamically impossible, but perhaps through mixing, small quantities of tracer are transported faster than actual parcels. Since the Lagrangian code derives temperatures by interpolation from the Eulerian fields, the conservation of parcel potential temperature is not to be expected. The midlatitude parcel simulation displayed much more moderate changes in potential temperature, indicating that it is a feature only of tropical motions in the model.

The CCM2 monthly mean 99-hPa tropopause is cooler than observed, but 99-hPa water vapor mixing ratios are somewhat too high. This may be due in part to an insufficient variance in very low temperatures and in part to the vertical resolution, which does not generally permit even resolved-scale convection to penetrate into the stratosphere while continuing to cool adiabatically. A strange consequence of the model's vertical velocity field is the association of strong downward motion with very low mixing ratio; this suggests that dry air is mostly recycled into the troposphere. The Lagrangian simulation does not offer strong proof of this; very few low-mixing ratio parcels returned to the troposphere after sharp dehydration during initial passage through the tropopause.

At higher vertical resolution, the tropopause moves up to around 85 hPa, and cross-tropopause mass flux drops by roughly a factor of 2 (although it remains the same at 100 hPa). Minimum mixing ratios drop, but their locations become less geographically fixed. While the minimum mixing ratio varies considerably, the zonal mean remains fairly constant near 2.4 ppmv throughout the year, although it is higher in northern fall.

Because the addition of the 85-hPa model level reduces tropopause temperatures and therefore water vapor mixing ratios, the zonal mean tropical water vapor distribution more closely resembles the observed. A model level there also reduces the variance (both spatial and temporal) in temperature and vertical velocity; as a result, the L35 resolution represents STE the best, by any measure other than zonal mean water vapor mixing ratio. The most likely cause of the inability of the CCM2 to reproduce observed features of tropical STE is that the CCM2 misrepresents the smallest-scale processes; in the atmosphere, mass transfer to the stratosphere occurs in convective systems whose horizontal scale is tens to thousands of kilometers and whose vertical scale (within the stratosphere) is hundreds of meters. The CCM2, with the resolution used here, smooths the smallest scales, and though producing reasonable area mean temperatures and vertical velocities, fails to capture the variance associated with these smallest scales.

In midlatitudes the CCM2 appears to be fairly successful in representing STE, indicating either that the important phenomena there are inherently of larger scale than the tropics or that the sub-grid-scale physics is better represented. Downward mass transfer occurs predominantly in conjunction with developing cyclones and stationary anticyclones, and upward mass transfer affects only the lowest couple of kilometers of the stratosphere. This finding sheds some light on the results of *Hoerling et al.* [1993] that large mass fluxes into the stratosphere occur in high latitudes. The density at the tropopause there can be nearly 3 times the density at the tropical tropopause, greatly exaggerating the importance of exchange there when it is evaluated relative to the tropopause; the 100-hPa surface is perhaps a more appropriate way to view stratosphere-troposphere exchange. If some mass transfer to the stratosphere does occur in mid-latitudes, it appears to be trapped below about 100 hPa, as supported both by our calculations and by trace constituent distributions.

The CCM2 is largely successful at simulating mass exchange both in the tropics and in the extratropics, despite a complete inability to represent the actual small-scale processes, which are particularly important in the former case. Exchange of trace gases, however, can be more problematic if their vertical gradients are large near the tropical tropopause. Modelers using GCMs to study tracer transport should be cautious in interpreting results near the tropical tropopause. In particular, GCM studies of aircraft emissions could be affected by misrepresented STE. It would be interesting to see if other GCMs share characteristics of STE with the CCM2.

Acknowledgments. Research supported by NASA Global Change Fellowship NGT 30076, NASA Grant NAGW-662, NSF grant ATM-8813971, and NASA Grant W18181 (NCAR).

References

Appenzeller, C., and H. C. Davies, Structure of stratospheric intrusions into the troposphere. *Nature, 358,* 570-572, 1992.

Balsley, B.B., W.L. Ecklund, D.A. Carter, A.C. Riddle and K.S. Gage, Average vertical motions in the tropical atmosphere observed by a radar wind profiler on Pohnpei (7°N latitude, 157°E longitude), *J. Atmos. Sci., 45,* 396-405, 1988.

Boville, B.A., J.R. Holton, and P.W. Mote, Simulation of the Pinatubo aerosol cloud in a general circulation model, *Geophys. Res. Lett., 18,* 2281-2284, 1991.

Brewer, A.W., Evidence for a world circulation provided by the measurement of helium and water vapour distribution in the stratosphere, *Q. J. R. Meteorol. Soc., 75,* 351-363, 1949.

Browell, E.V., E.F. Danielsen, S. Ismail, G.L. Gregory, and S.M. Beck, Tropopause fold structure determined from airborne lidar and in situ measurements, *J. Geophys. Res., 92,* 2112-2120, 1987.

Danielsen, E.F., Stratospheric-tropospheric exchange based on radioactivity, ozone and potential vorticity, *J. Atmos. Sci., 25,* 502-518, 1968.

Danielsen, E.F., A dehydration mechanism for the stratosphere, *Geophys. Res. Lett., 9,* 605-608, 1982.

Danielsen, E.F., In situ evidence of rapid, vertical, irreversible transport of lower tropospheric air into the lower tropical stratosphere by convective cloud turrets and by larger-scale upwelling in tropical cyclones, *J. Geophys. Res., 98,* 8665-8682, 1993.

Danielsen, E.F., R.S. Hipskind, S.E. Gaines, G.W. Sachse, G.L. Gregory, and G.F. Hill, Three-dimensional analysis of potential vorticity associated with tropopause folds and observed variations of ozone and carbon monoxide, *J. Geophys. Res., 92,* 2103-2111, 1987.

Dobson, G.M.B., Origin and distribution of polyatomic molecules in the atmosphere, *Proc. R. Soc. London, A236,* 187-193, 1956.

Doherty, G.M., R.E. Newell, and E.F. Danielsen, Radiative heating rates near the stratospheric fountain, *J. Geophys. Res., 89,* 1380-1384, 1984.

Frederick, J.E., and A.R. Douglass, Atmospheric temperatures near the tropical tropopause: Temporal variations, zonal asymmetry and implications for stratospheric water vapor, *Mon. Weather Rev., 111*, 1397-1403, 1983.

Garcia, R.R., and S. Solomon, A numerical model of the zonally averaged dynamical and chemical structure of the middle atmosphere, *J. Geophys. Res. 88*, 1379-1400, 1983.

Hack, J.J., Parameterization of moist convection in the National Center for Atmospheric Research Community Climate Model (CCM2). *J. Geophys. Res. 99*, 5551-5568, 1994.

Hack, J.J., B.A. Boville, B.P. Briegleb, J.T. Kiehl, P.J. Rasch, and D.L. Williamson, Description of the NCAR Community Climate Model (CCM2), *NCAR Tech.Note NCAR/TN-382+STR*, Nati .Cent. for Atmos. Res., Boulder, Colo.,1993.

Haynes, P.H., C.J. Marks, M.E. McIntyre, T.G. Shepherd, and K.P. Shine, On the "downward control" of extratropical diabatic circulations by eddy-induced mean zonal forces, *J. Atmos. Sci., 48*, 651-678, 1991.

Hoerling, M.P., T.K. Schaack, and A.J. Lenzen, A global analysis of stratospheric-tropospheric exchange during northern winter. *Mon. Weather. Rev., 121*, 162-172, 1993.

Holton, J.R., Troposphere-stratosphere exchange of trace constituents: The water vapor puzzle, in *Dynamics of the Middle Atmosphere*, edited by J.R. Holton and T. Matsuno, pp. 369-385, Terrapub., Scientific, Tokyo, 1984.

Holton, J.R., On the global exchange of mass between the stratosphere and troposphere, *J. Atmos. Sci. 47*, 392-395, 1990.

Johnston, H.S., and S. Solomon, Thunderstorms as possible micrometeorological sink for stratospheric water, *J. Geophys. Res. 84*, 3155-3158, 1979.

Jones, R. L., and J. A. Pyle, Observations of CH_4 and N_2O by the Nimbus 7 SAMS: A comparison with in situ data and two-dimensional numerical model calculations, *J. Geophys. Res., 89*, 5263-5279, 1984.

Kelly, K.K., M. H. Proffitt, K.R. Chan, M. Loewenstein, J.R. Podolske, S.E. Strahan, J.C. Wilson, and D. Kley, Water vapor and cloud water measurements over Darwin during the STEP 1987 tropical mission, *J. Geophys. Res., 98*, 8713-8724, 1993.

Kley, D., A.L. Schmeltekopf, K. Kelly, R. H. Winkler, T.L. Thompson, and M. McFarland, Transport of water through the tropical tropopause, *Geophys. Res. Lett., 9*, 617-620, 1982.

Knollenberg, R.G., K.K. Kelly, and J.C. Wilson, Measurements of high number densities of ice crystals in the tops of tropical cumulonimbus, *J. Geophys. Res., 98*, 8639-8664, 1993.

Kritz, M.A., S.W. Rosner, E.F. Danielsen, and H.B. Selkirk, Air mass origins and troposphere-to-stratosphere exchange associated with midlatitude cyclogenesis and tropopause folding inferred from ^7Be measurements, *J. Geophys. Res., 96*, 17,405-17,414, 1991.

Kritz, M.A., S.W. Rosner, K.K. Kelly, M. Loewenstein, and K.R. Chan, Radon measurements in the lower tropical stratosphere: Evidence for rapid vertical transport and dehydration of tropospheric air, *J. Geophys. Res., 98*, 8725-8736, 1993.

Newell, R.E., and S. Gould-Stewart, A stratospheric fountain? *J. Atmos. Sci., 38*, 2789-2796, 1981.

Randel, W.J., Global atmospheric circulation statistics, 1000-1 mb, *NCAR Tech. Note, NCAR/TN-366+STR*, NCAR, Boulder, Colo.,1992.

Reed, R.J., and E.F. Danielsen, Fronts in the vicinity of the tropical tropopause. *Arch. Meteorol. Geophys. Bioklim., 11*, 1-17, 1959.

Reid, G.C., and K.S. Gage, On the annual variation in the height of the tropical tropopause, *J. Atmos. Sci. 38*, 1928-1938, 1981.

Rind., D., E.-W. Chiou, W. Chu, S. Oltmans, J. Lerner, J. Larsen, M.P. McCormick, and L. McMaster, Overview of the stratospheric aerosol and gas experiment II water vapor observations: Method, validation, and data characteristics, *J. Geophys. Res., 98*, 4835-4856, 1993.

Robinson, G.D., and M.G. Attieks Schoen, The formation and movement in the stratosphere of very dry air, *Q. J. R. Meteorol. Soc., 113*, 653-679, 1987.

Rosenlof, K.H., and J.R. Holton, Estimates of the stratospheric residual circulation using the downward control principle, *J. Geophys. Res., 98*, 10,465-10,479, 1993.

Russell, P.B., L. Pfister, and H. B. Selkirk, The tropical experiment of the Stratosphere-Troposphere Exchange Project (STEP): Science objectives, operations, and summary findings, *J. Geophys. Res., 98*, 8563-8590, 1993.

Selkirk, H.B., The tropopause cold trap in the Australian monsoon during STEP/AMEX 1987, *J. Geophys. Res., 98*, 8591-8610, 1993.

Trepte, C.R., R.E. Veiga, and M.P. McCormick, The poleward dispersal of Mt. Pinatubo volcanic aerosol, *J. Geophys. Res., 98*, 18563-18573, 1993.

Yulaeva, E., J.R. Holton, and J.M. Wallace, On the cause of the annual cycle in tropical lower stratospheric temperatures, *J. Atmos. Sci. 51*, 169-174, 1994.

Zhang, C., Large-scale variability of atmospheric deep convection in relation to sea surface temperature in the tropics, *J. Clim. 6*, 1898-1913, 1993.

B. A. Boville, National Center for Atmospheric Research, P.O. Box 3000, Boulder, CO 80307.

J. R. Holton, Department of Atmospheric Sciences, AK-40, University of Washington, Seattle, WA 98195.

P. W. Mote (corresponding author), Department of Meteorology, University of Edinburgh, King's Buildings, Edinburgh EH9 3JZ, Scotland, U. K. (e-mail: mote@met.ed.ac.uk)

(Received October 6, 1993; revised February 12, 1994;
accepted April 1, 1994.)